Acta Cryst. (1972). B28, 1211

The Crystal Structure of the *X* Phase (Mn,Co,Si)

BY PHILIP C. MANOR,* CLARA BRINK SHOEMAKER,† AND DAVID P. SHOEMAKER†

Department of Chemistry, Massachusetts Institute of Technology, Cambridge, Massachusetts 02139, *U.S.A.*

(*Received* 29 *July* 1971)

The crystal structure of the intermetallic compound $Mn_{45}Co_{40}Si_{15}$, known as *X* phase (and also as *Y* phase), has been determined by direct methods from data collected on an automated single-crystal X-ray diffractometer, and has been refined by least-squares methods to a conventional *R* index of 0·070, based on 1597 observed reflections. The structure is orthorhombic, space group *Pnnm*, with lattice constants $a = 15{\cdot}42\ (2)$, $b = 12{\cdot}39\ (2)$, $c = 4{\cdot}74\ (1)$ Å [λ(Mo $K\alpha_1$) = 0·70926 Å], and with 74 atoms per unit cell; $\varrho_{exp} = 7{\cdot}08\ (14)$, $\varrho_{cal} = 7{\cdot}12$ g.cm^{-3}. In a manner resembling a number of other σ-phase related compounds, the *X*-phase structure is layered, with two main layers and two subsidiary layers per *c*-axis repeat. The *X*-phase structure can be regarded as an extension of the structure types represented by Zr_4Al_3, $MgCu_2$(*C*15), and $MgZn_2$(*C*14), in that all four of these alloys can be considered as aggregates of infinite pentagonal antiprism columns (*i.e.* columns of fused icosahedra) with the maximum number of shared pentagon sides per pentagon (in a 'main layer' perpendicular to the columns) increasing according to the sequence 1,2,3,4 for the alloys Zr_4Al_2, $MgCu_2$, $MgZn_2$, and *X* phase respectively. The percentages of sites with coordination number 12, 14, 15, and 16 in the *X* phase are, respectively: 63, 5, 5, and 27. After submitting this paper, the authors learned that Yarmolyuk, Kripyakevich & Hladyshevskii [*Kristallografiya* (1970), **15**, 268; *Sov. Phys. Crystallogr.* **15**, 226] obtained, with photographic data (refining only with *hk*0), an essentially similar structure for the *X* phase, differing only in values of interatomic distances and site compositions.

Introduction

The existence of the *X* phase was first revealed by Kuz'ma (1962) in an examination of the 800 °C section of the Mn, Co, Si ternary system at a composition of $Mn_{40-35}Co_{45-50}Si_{15}$, later revised by Kuz'ma and Hladyshevskii (1964) to $Mn_{45-40}Co_{40-45}Si_{15}$. Bardos, Malik, Spiegel & Beck (1966), in an investigation of the 1000°C section of the Mn, Co, Si system, reported a new '*Q* phase' at nearly the same composition, $Mn_{45}Co_{40}Si_{15}$, and also reported the existence of a *Y* phase at a composition near $Mn_{39}Co_{42}Si_{19}$. These authors noted, on the basis of a comparison of powder X-ray diffraction patterns, the probable identity of the *Y* phase with the *X* phase.

From a '*Q* phase' sample of bulk composition $Mn_{45}Co_{40}Si_{15}$, annealed at 1000 °C and kindly provided by Professor Paul A. Beck, five crystal fragments, apparently identical in structure as indicated by single-crystal X-ray diffraction photography, were isolated. It was initially assumed that the isolated material was representative of the material we knew as '*Q* phase'. However, later comparison of the powder diffraction pattern calculated from the refined structure found for the single-crystal material, with the reported experimentally determined diffraction patterns of *X*, *Y*, and *Q* phases, indicated that all the isolated single-crystal material was isostructural with the *X* phase or *Y* phase. The correspondence between the calculated pattern and the patterns reported for the *X* and *Y* phases is given in Table 1; the calculated pattern is based on cell constants obtained by unconstrained least-squares refinement of diffractometer measurements and on approximate thermal, occupancy, and positional parameters. It was not possible to place the reported *Q*-phase diffraction pattern in similar detailed correspondence with the calculated pattern; material designated '*Q* phase' is evidently a mixture of *X* phase with one or more additional phases.

The chemical composition of the small single crystals obtained from the bulk sample was determined both by electron microprobe and by wet chemical analysis. An elongated prismatic fragment was isolated from an aggregate of morphologically similar fragments and was examined by single-crystal X-ray photographic methods. The fragment was found to be a single crystal of *X* phase, elongated in the *c*-axis direction. Electron microprobe analysis of the aggregate, approximately 2 mm in diameter, detected no apparent chemical inhomogeneity and gave a chemical composition of approximately $Mn_{45}Co_{42}Si_{13}$. A more precise determination of the aggregate's chemical composition, afforded by standard wet chemical techniques, gave $Mn_{44.4}Co_{40.0}Si_{15.1}$. This composition is in accord with the overall bulk composition of the sample ($Mn_{45}Co_{40}Si_{15}$) from synthesis, and is within the limits specified for the *X* phase in the 800 °C section. This again leads to the conclusion that the so-called '*Q* phase' actually is an, as yet, unidentified mixture of phases,

* This work is described in a thesis submitted in partial fulfillment of the requirement for the Ph.D degree at the Massachusetts Institute of Technology, January, 1971. Present address: Max-Planck-Institut für experimentelle Medizin, 34, Göttingen, B.R.D.

† Present address: Department of Chemistry, Oregon State University, Corvallis, Oregon, 97331, U.S.A.

with the *X* phase as one constituent; the possibility that a major portion of the mixture is a previously unidentified phase that might be named '*Q* phase' cannot be excluded.

Experimental

Single-crystal Weissenberg and precession photographs indicate that the structure is orthorhombic with systematic extinctions corresponding to space groups *Pnnm* (D_{2h}^{12}, No. 58) and *Pnn*2 (C_{2v}^{10}, No. 34). As refinement was satisfactory in the centrosymmetric group *Pnnm*, no further consideration was given to the lower space group. Table 2 gives the relevant crystal data; the lattice constants were obtained from (unconstrained) least-squares refinement of diffractometer measurements, and the density was measured experimentally with a pycnometer by methanol displacement.

The structure was deduced through the application of the symbolic addition direct sign-determining method (Karle & Hauptman, 1953; Karle & Karle, 1966), operating on a provisional, visually estimated data set of 347 reflections from Weissenberg photographs of levels $l=0,1,2$. By using the reflections 14,8,1, 232, 952 as origin symbols (plus) with additional reflections 382 and 251 (assigned minus) and by applying the $\sum_2$ relation, it was possible to generate the signs of 171 other reflections. An *E* map, taken perpendicular to the *c* axis (section at $z=0$), quickly revealed the structure, and later comparison indicated that 77% of the 171 sign assignments were correct. While this percentage is much lower than is usually expected for a successful application of this method, it was surprising that the method worked so easily for a structure of this kind, in which the dense packing of atoms leads to very non-statistical distributions of intensities in reciprocal space. Moreover, only three reciprocal lattice layers were used, since intensities in all other layers are related to these by the layering of the structure.

With an irregularly shaped *X*-phase crystal specimen

Table 1. *A comparison of the powder pattern computed from single-crystal data with the patterns of X phase and Y phase**

Line		Calculated		*Y* phase†		*X* phase‡	
number	*h k l*	*d*(Å)	*I*(rel)	*d*(Å)	*I*(rel)	*d*(Å)	*I*(rel)
0	3 1 0	4·7469	36				
1	1 3 0	3·9891	10	3·949	1		
	3 2 0	3·9552	56				
2	4 0 0	3·8543	23	3·849	0·5		
3	2 3 0	3·6403	63	3·636	1		
4	4 2 0	3·2725	46	3·261	0·5		
5	0 4 0	3·0973	13	3·093	0·5		
6	3 2 1	3·0369	39	3·036	1		
	1 4 0	3·0366	9				
7	1 4 1	2·5570	46	2·552	0·5		
8	0 0 2	2·3701	201	2·373	2	2·383	1
9	1 1 2	2·3018	12	2·315	0·5		
				2·266	0·5		
10	2 1 2	2·2285	16	2·231	0·5	2·244	1
11	5 3 1	2·1910	917	2·186	7	2·203	4
12	2 5 1	2·1119	1000	2·090	11	2·127	4
13	7 2 0	2·0752	575	2·069	7	2·079	3
	0 6 0	2·0649	177				
14	1 6 0	2·0466	95	2·033	5		
	1 3 2	2·0376	117				
	3 2 2	2·0330	291				
15	4 0 2	2·0189	358	2·018	3		
16	7 0 1	1·9974	591	1·989	12	1·995	5
	4 1 2	1·9926	153				
	2 3 2	1·9862	987				
17	6 3 1	1·9819	64				
	6 4 0	1·9776	67				
18	5 5 0	1·9315	537	1·927	4	1·940	3
19	4 2 2	1·9196	28	1·899	0·5		
	3 6 0	1·9160	40				
	3 3 2	1·9086	39				
	8 1 0	1·9043	36				
20	0 4 2	1·8822	53	1·882	0·5		
21	1 4 2	1·8684	49	1·856	2	1·861	2
	5 1 2	1·8579	212				
22	2 6 1	1·8384	28	1·819	0·5	1·831	1
	2 4 2	1·8285	31				
	6 4 1	1·8251	54				
	4 6 0	1·8201	65				
23	5 2 2	1·7982	17	1·790	0·5		
	7 4 0	1·7949	27				

Table 1 (*cont.*)

Line		Calculated		*Y* phase†		*X* phase‡	
number	*h k l*	*d*(Å)	*I*(rel)	*d*(Å)	*I*(rel)	*d*(Å)	*I*(rel)
24	3 6 1	1·7764	78	1·775	1		
25	8 3 0	1·7464	27	1·739	0·5		
26	2 7 0	1·7250	88	1·723	1	1·727	1
27	1 5 2	1·7023	38	1·695	0·5	1·704	1
	4 6 1	1·6992	21				
	9 1 0	1·6969	43				
28	7 4 1	1·6786	28	1·673	0·5	1·681	1
	6 2 2	1·6771	17				
29	9 1 2	1·3797	25	1·378	0·5		
	4 8 1	1·3752	34				
30	5 3 3	1·3311	125	1·331	2	1·332	2
31	2 5 3	1·3128	153	1·312	2	1·316	3
32	10 0 2	1·2924	64	1·290	1		
33	7 0 3	1·2839	123	1·284	2	1·286	3
34	7 8 0	1·2668	134	1·264	3	1·269	3
35	3 8 2	1·2570	179	1·256	3	1·259	4
36	4 9 1	1·2505	33	1·249	1		
37	0 10 0	1·2389	65	1·237	3	1·241	1
	2 6 3	1·2385	13				
	10 6 0	1·2354	14				
38	6 4 3	1·2344	16	1·231	2	1·235	1
	12 1 1	1·2339	51				
39	12 3 0	1·2268	132	1·224	3	1·228	3
	3 6 3	1·219	33				
40	9 5 2	1·2112	340	1·210	7	1·211	5
41	0 0 4	1·1851	163			1·184	4
	11 2 2	1·1842	47				
42	3 10 1	1·1673	26			1·158	3
	3 9 2	1·1597	63				

* The *Y*-phase line given here as 2·090 Å, matching the calculated 2·1119 Å line, is given as 2·190 Å in Bardos *et al.* (1966). In that reference a line at 2·190 is an exception to a monotonically decreasing sequence, and further is associated with an *X*-phase line at 2·127; therefore, it appears that 2·190 should have been 2·090. Other minor changes in the correspondence between the *X*- and *Y*-phase patterns have been made. In general, all calculated lines with an intensity <25 have been deleted, except for those cases where weak lines overlap adjacent lines to produce or change the intensity of an observable line.

† Bardos *et al.* (1966).

‡ Kuz'ma (1962).

Table 2. *Crystal data*

Composition (chemical analysis)	Weight %	Atomic %
Manganese	46·6	44·4
Cobalt	44·9	40·0
Silicon	8·1	15·1

Systematic absences	$0kl: k+l\neq 2n$; $h0l: h+l\neq 2n$
Space group	*Pnnm*, No 58, D_{2h}^{12}
a	15·417 (20) Å
b	12·389 (20)
c	4·740 (10)
V	905 (4) Å^3
Z	74 atoms per unit cell
D_{exp}	7·08 (14) g.cm^{-3}
D_{calc}	7·12 g.cm^{-3}
Radiation	Mo $K\alpha$, 0·70926 Å (α_1)

Linear absorption coefficient $\mu=256$ cm^{-1}

Mass absorption coefficient $\mu/\varrho=35{\cdot}91$ cm^{2}g^{-1}

(approximately 0·155 mm in the largest dimension and 0·05 mm in the smallest) placed in an arbitrary orientation on a Datex (tape) automated G. E. diffractometer, 2993 intensity measurements were made in a single octant of reciprocal space out to $2\theta=75°$. These measurements were made using Zr-filtered Mo $K\alpha$ radiation and the θ–2θ scan method, with stationary-crystal stationary-counter background measurements of 40 sec both at the beginning and the end of each scan. After approximately every 60 measurements, the intensities of the standard reflections 720, 060, and 004 were measured; they showed no significant variation. With the standard deviation of the intensity estimated from $\sigma(I)=[(C+T^2B)/10+(0{\cdot}01\ I)^2]^{1/2}$ (where T = scanning time/total background time), based on counting statistics plus a 1% instrumental error allowance, the

979 reflections with intensities less than 2·5 $\sigma(I)$ were deleted. The least-squares refinement was based on the intensities of 1597 observed independent reflections, excluding 40 very strong reflections with $F_o < F_c$, presumably owing to secondary extinction. Attempts to correct the data for absorption, using either numerical integration or the polyhedron method, were unsuccessful, presumably because of the very complicated shape of the crystal as shown by scanning electron microscope photographs. A spherical absorption correction was applied with $\mu r = 1{\cdot}3$, corresponding to transmission factors ranging from 0·164 to 0·202.

Refinement

During the initial stages of least-squares refinement, it became apparent that the silicon atoms were not uniformly distributed by substitutional disorder among CN12 positions, but instead were mainly confined to four kinds of such positions, three of which appeared to contain mainly silicon, the fourth containing a significantly smaller proportion of silicon. As only one occupancy factor can be satisfactorily refined for each position, the chemical composition at each site in a ternary alloy cannot be determined from X-ray data alone without certain simplifying assumptions. The composition of the *X* phase indicates that the 74 atoms of the unit cell comprise 33 manganese, 30 cobalt, and 11 silicon atoms. It was assumed that the 28 atoms corresponding to positions with coordination number greater than 12 were manganese, because in other σ-phase related phases 'B' atoms, such as cobalt, are not normally found with coordination number greater than 12. A weighted average scattering factor for the CN12 sites not occupied by silicon was then computed from $f_{\mathrm{CoMn}} = (1/39)\,(9f_{\mathrm{Mn}} + 30f_{\mathrm{Co}})$.*

The effective multiplicities (containing occupancy factors) for the four atom sites containing silicon were then refined. The scattering factors used for this procedure were f_{Si} for the three sites that appeared to contain mainly silicon, and f_{CoMn} for the one site that initially appeared to contain a lesser proportion of silicon. From the ratio of the refined to the crystallographic multiplicity, the implied chemical composition was computed (Table 3). All scattering factors were taken from the *International Tables for X-ray Crystallography* (1962) and were corrected for the real part of the dispersion correction taken from the same source. (These corrections are not made in Z_{app}, listed in Table 3, which was calculated from m_{obs}.) The quan-

Table 3. *X phase atomic parameters*

CN	Atom	No.	Site	*x*	*y*	*z*	*B*	m_c	m_{obs}	Z_{app}	Atoms per unit cell Mn	Co	Si
12	CoMn	1	8(*h*)	0·1106 (1)	0·0858 (1)	0·2428 (4)	0·42 (2)	1·0	1·0	26·7	1·14	6·86	
12	CoMn	2	8(*h*)	0·1759 (1)	0·3980 (1)	0·2354 (4)	0·48 (2)	1·0	1·0	26·7	1·14	6·86	
12	CoMnSi	3	8(*h*)	0·3981 (1)	0·2104 (1)	0·2536 (6)	0·46 (3)	1·0	0·798 (7)	21·3	0·66	3·94	3·40
12	Si	6	4(*g*)	*m*	0·2156 (3)	0·9917 (3)	0	0·48 (8)	0·5	0·57 (1)	16·0	0·09	0·54	3·37
12	CoMn	7	4(*g*)	*m*	0·3607 (1)	0·0573 (2)	0	0·43 (3)	0·5	0·5	26·7	0·57	3·43	
12	CoMn	8	4(*g*)	*m*	0·4986 (2)	0·3107 (2)	0	0·42 (3)	0·5	0·5	26·7	0·57	3·43	
12	Si	10	2(*b*)	2/*m*	½	0	0·52 (12)	0·25	0·273 (7)	15·3	0·03	0·17	1·80	
12	Si	16	4(*g*)	*m*	0·3546 (3)	0·7424 (3)	0	0·61 (7)	0·5	0·622 (11)	17·4	0·15	0·92	2·93
12	CoMn	17	4(*g*)	*m*	0·2092 (2)	0·8023 (2)	0	0·43 (3)	0·5	0·5	26·7	0·57	3·43	
14	Mn	14	4(*g*)	*m*	0·0701 (2)	0·5292 (2)	0	0·54 (3)	0·5	0·5	25·0	4·00		
15	Mn	19	4(*g*)	*m*	0·4728 (2)	0·8993 (2)	0	0·50 (3)	0·5	0·5	25·0	4·00		
16	Mn	4	4(*g*)	*m*	0·0551 (2)	0·2779 (2)	0	0·61 (4)	0·5	0·5	25·0	4·00		
16	Mn	5	4(*g*)	*m*	0·2360 (2)	0·2130 (2)	0	0·60 (4)	0·5	0·5	25·0	4·00		
16	Mn	9	4(*g*)	*m*	0·3394 (2)	0·3990 (2)	0	0·57 (3)	0·5	0·5	25·0	4·00		
16	Mn	15	4(*g*)	*m*	0·2351 (2)	0·5865 (2)	0	0·50 (4)	0·5	0·5	25·0	4·00		
16	Mn	18	4(*g*)	*m*	0·0506 (2)	0·9026 (2)	0	0·54 (3)	0·5	0·5	25·0	4·00		
										Total	32·92	29·58	11·50
										=	74·00		
										Atomic %	44·5	40·0	15·5

* This expression was constructed from an erroneous atomic ratio, Mn: Co = 9:30, for these sites. the correct expression, based on the actual ratio of 5:30, should have been $(1/35) \times (5f_{\mathrm{Mn}} + 30f_{\mathrm{Co}})$. The two expressions are closely similar, numerically, giving 26·5 and 26·7 respectively for the scattering factor (Z_{app}) at $2\theta = 0°$. The error was found too late for it to be corrected in advance of the final least-squares refinement, but the site compositions given in Table 3, and the m_{obs} value given for CoMnSi, have been adjusted on an electron-count basis.

Table 4. *Observed* (*left column*) *and calculated* (*right column*) *structure factors for the X phase*

*='un-observed', (=systematic absence, E=secondary extinction. All marked reflections were omitted from the final least-squares refinement.

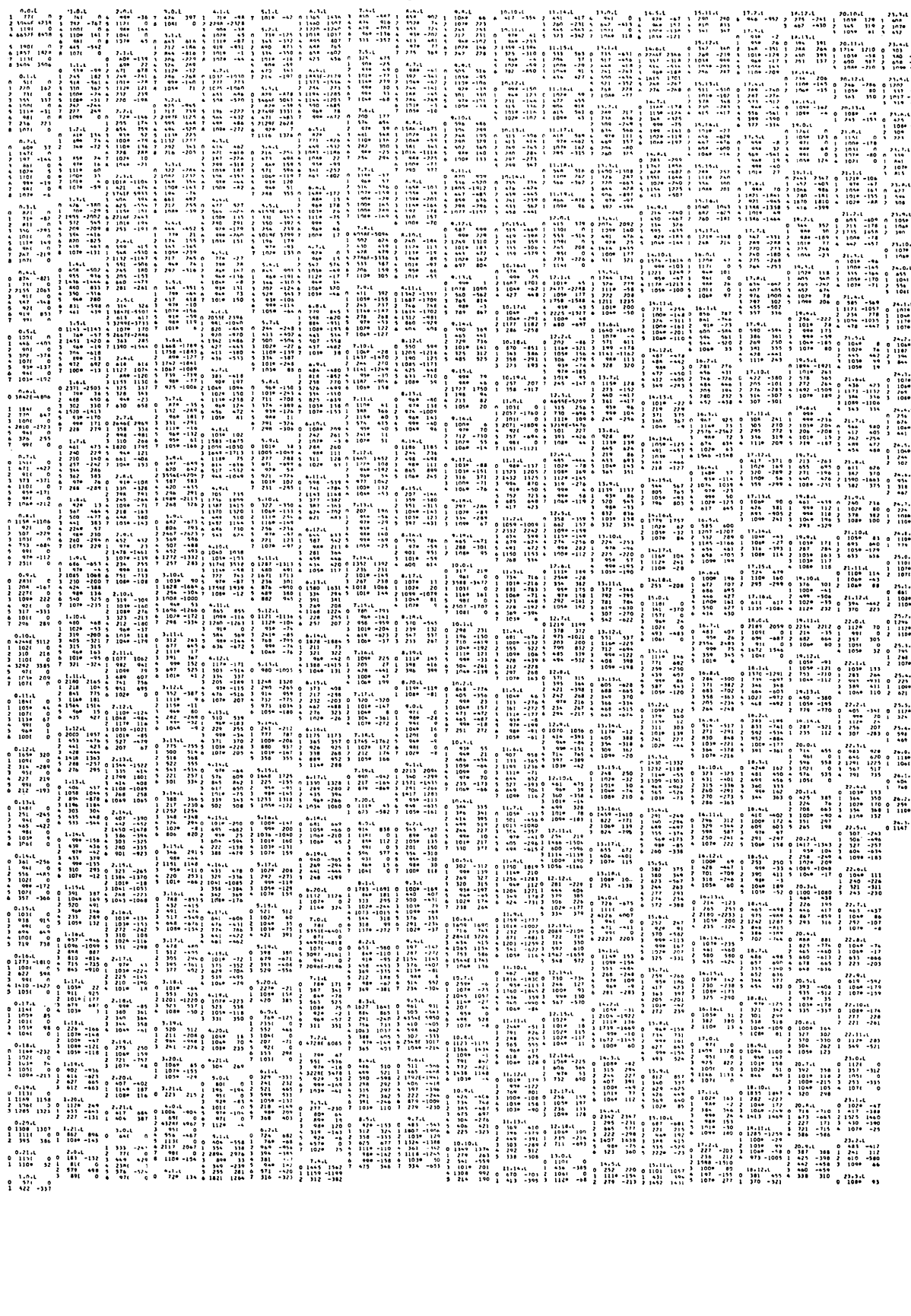

tity minimized was $\sum w(|F_o|-|F_c|)^2$, using for weights $1/[\sigma(F)]^2$ derived from the previously given expression for $\sigma(I)$. Both an isotropic and an anisotropic model were refined, and the anisotropic model was rejected because of the statistically insignificant decline in the R index that resulted, and because of the likelihood of uncorrected anisotropic absorption effects. The final agreement indices, taken over all observed reflections, were $R_1 = 0{\cdot}070 = \sum||F_o|-S|F_c||/\sum|F_o|$ and $R_2 = 0{\cdot}074 = [\sum w(|F_o|-|SF_c|)^2/\sum w|F_o|^2]^{1/2}$. The final atomic parameters are listed in Table 3 and the comparisons of F_o and F_c are given in Table 4. (F_o for unobserved reflections and systematic extinctions is given as 0·5 F_{min}.)

Discussion

In a manner resembling a large number of other σ-phase related intermetallic compounds in which all interstices are tetrahedral, the X phase structure is layered, with four layers per c-axis repeat. Fig. 1 is a projection of the structure onto the x-y plane; the net at $z=0$ is indicated by solid lines, the net at $z=\frac{1}{2}$ by broken lines, and atoms at approximately $z=0{\cdot}25$ and $z=0{\cdot}75$ are indicated by filled-in circles. The size of the circles increases with increasing coordination number of the atoms. The only types of coordination polyhedra found are the ones normally found in various combinations in σ-phase related phases, namely those

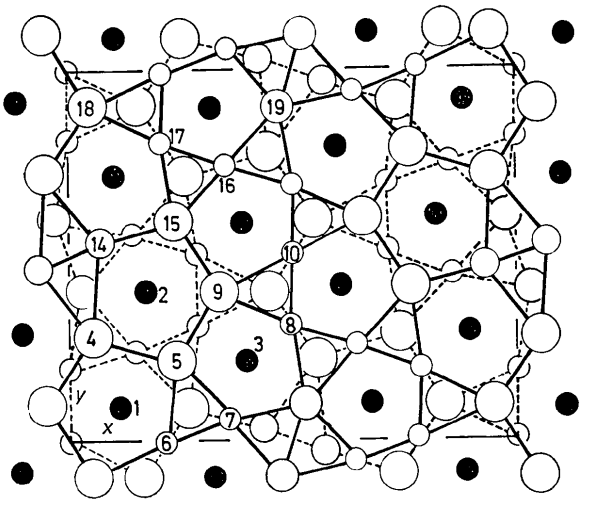

Fig. 1. Projection of the X-phase structure onto the x–y plane. The net at $z=0$ is indicated by solid lines, the net at $z=\frac{1}{2}$ by broken lines. Filled-in circles are atoms at approximately $\frac{1}{4}$ and $\frac{3}{4}$. The sizes of the circles increase with increasing coordination number of atoms.

having the coordinations and idealized symmetries CN12 ($\bar{5}\,.\,\bar{3}\,.\,2/m$), CN14 ($\bar{1}\bar{2}\,.\,2\,.\,m$), CN15 ($\bar{6}m2$), and CN16 ($\bar{4}3m$) (see Shoemaker & Shoemaker, 1968).

Each of the pentagons in the main layers may be regarded as a section through an icosahedral coordi-

Table 5. *Interatomic distances*

The superscript numerals indicate the number of times a distance occurs when reading down, and an asterisk indicates a 'major ligand' distance. The standard deviations given by the refinement range between 0·003 and 0·006 Å.

No.	CN	1 12	2 12	3 12	6 12	7 12	8 12	10 12	16 12	17 12	14 14	19 15	4 16	5 16	9 16	15 16	18 16
1	12	2.438 2.302			2.302^2		2.472^2	2.350^4	2.355^2				2.797^2	2.747^2	2.727^2	2.672^2	2.708^2 2.742^2
2	12		2.508 2.332		2.393^2	2.406^2			2.346^2	2.474^2	2.560^2	2.612^2	2.632^2	2.712^2	2.758^2	2.745^2	
3	12			2.430 2.310		2.325^2	2.328^2			2.316^2	2.572^2	2.700^2	2.686^2	2.779^2	2.784^2	2.812^2	2.762^2
6	12	2.302	2.393			2.381				2.349				2.759	2.767^2	2.752^2	2.773
7	12		2.406	2.325	2.381						2.622^2	2.611 2.623		2.724		2.816^2	
8	12	2.472		2.328				2.345^2	2.358			2.639	2.753^2		2.686		2.736^2
10	12	2.350					2.345								2.774		2.771^2
16	12	2.355	2.346				2.358			2.361		2.669	2.784^2	2.775^2		2.669	
17	12		2.474	2.316	2.349				2.361					2.749^2	2.759^2	2.703	2.743
14	14		2.560	2.572		2.622^2					2.279*	2.941^2 2.940^2	3.122 3.071			2.642*	
19	15		2.612	2.700		2.611 2.623	2.639		2.669		2.941^2 2.940^2	2.632*	2.839$^2_*$				
4	16	2.797	2.632	2.686			2.753^2		2.784^2		3.122 3.071	2.839$^2_*$		2.903*			2.766*
5	16	2.747	2.712	2.779	2.759	2.724			2.775^2	2.749^2			2.903*		2.802*	2.876$^2_*$	
9	16	2.727	2.758	2.784	2.767^2		2.686	2.774^2		2.759^2				2.802*		2.825*	2.914$^2_*$
15	16	2.672	2.745	2.812	2.752^2	2.816^2			2.669	2.703	2.642*			2.876$^2_*$	2.825*		
18	16	2.708 2.742		2.762	2.773		2.736^2	2.771^4		2.743			2.766*		2.914$^2_*$		2.874*
		CoMn	CoMn	CoMnSi	Si	CoMn	CoMn	Si	Si	CoMn	Mn	Mn	Mn	Mn	Mn	Mn	Mn

nation polyhedron centered on one of the atoms of the subsidiary layers or, alternatively, as a section through an infinite pentagonal-antiprism column whose axis passes through atoms of the secondary layers parallel to **c**. Infinite pentagonal-antiprism columns occur in other tetrahedrally close-packed structures, sometimes combined with infinite hexagonal-antiprism columns (as in *P* phase and *v* phase). In the *X* phase, the coordination polyhedra around all the secondary-layer atoms have pentagonal sections in the main layers, which is also true for the *M* phase, the μ phase (when viewed along [110]), Zr_4Al_3 (viewed along [110]), and the Friauf–Laves phases $MgCu_2$ (along $[1\bar{1}0]$) and $MgZn_2$ (along [110]). As regards the association of one pentagon with another within a layer, the *X* phase is an extension of the previously known structure types. In Zr_4Al_3, every main-layer pentagon shares a side with only one other pentagon; in $MgCu_2$ every such pentagon has two sides in common with other pentagons, and in $MgZn_2$ each pentagon is surrounded by, at most, three others (Shoemaker & Shoemaker, 1968). In the X phase, three different types of pentagons are found, which share respectively one, three, and the unusual number of four, sides with surrounding pentagons. This unusual arrangement of atoms in the primary layers is reflected in the unusual secondary-layer tessellation pattern, where, in Schläfli notation, the forms 4.3^5 and 4.3^4 are found (Fig. 2). These forms are not among the types discussed by Frank & Kasper (1958, 1959).

The tessellations 4.3^5 and 4.3^4 cannot occur with equilateral triangles and squares. As previously pointed out (Shoemaker & Shoemaker, 1969), the triangles formed by the secondary atoms in structures containing pentagons in the main layers are not equilateral, but have one angle of about 70° and two angles of about 55° and the quadrilaterals are rectangles with sides of two different lengths. Thus, a 3^6 tessellation is formed by four angles of approximately 55°and two angles of 70° (atom 1 in the *X* phase). A tessellation $3^4.4$ (atom 2 in the *X* phase) is thus possible with 3 angles of approximately 70°, one of about 55°, and one of about 90°; a tessellation $3^5.4$ (atom 3 in the *X* phase) occurs by joining five angles of about 55° and one angle of about 90°. Fig. 2 shows how a secondary net is constructed by combining these three types of tessellations, forming triangles and rectangles of the same type and not very much more distorted than those found in other tetrahedrally close-packed structures. Hence, the coordination polyhedra in the *X* phase have about the same degree of distortion as those in other tetrahedrally close-packed structures, even though the structure does not fall under the classification scheme described by Pearson & Shoemaker (1969). That scheme covers only those structures whose secondary nets can be generated by two sets of parallel lines, leading to secondary net tessellations of the types 4^4, 3^6, $4.3.4.3^2$ and $4^2.3^3$ only.

In the *X* phase, as in other layered phases of this type, atoms in the secondary layer are not confined by symmetry to planes at $z=0{\cdot}25$ and $z=0{\cdot}75$; atom 1 is displaced downward from $z=0{\cdot}25$ by 0·034 Å, atom 2 downward by 0·069 Å, and atom 3 upward by 0·030

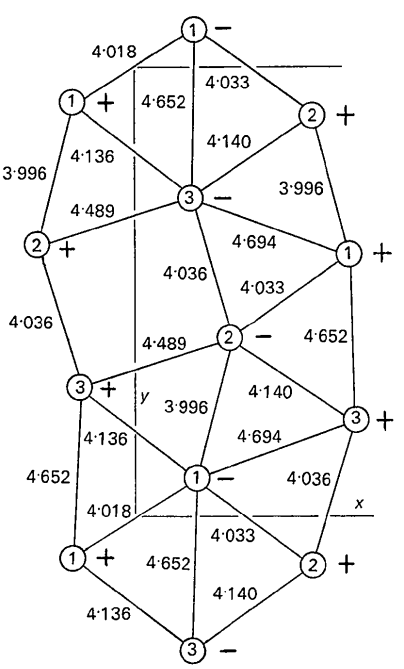

Fig. 2. Secondary-layer tessellation. Distances are given in Å, and the vertical displacements (relative to $z=\frac{1}{4}$) are indicated by plus and minus signs.

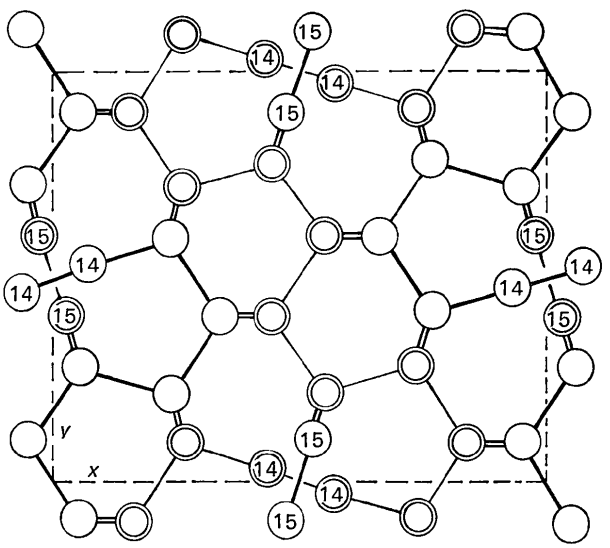

Fig. 3. 'Major network' for *X* phase. Single circles represent atoms on layer $z=0$; double circles represent atoms on layer $z=\frac{1}{2}$. Single lines represent major ligands between atoms in the same main layer; double lines represent major ligands between atoms in two adjacent main layers, and thus represent two ligands per atom. All atoms are CN16 except those with CN14 or CN15 which are marked accordingly.

Å (all with e.s.d.'s of approximately 0·005Å). These displacements are larger than in most such phases, but comparable to the largest (0·058 Å) found in the *v* phase (Shoemaker & Shoemaker, 1971). They result in CN12–CN12 interatomic distances as long as 2·508 Å and as short as 2·232 Å, compared to the mean CN12–CN12 distance of 2·37 (1) Å. With this exception, all other *X*-phase interatomic distances appear normal for phases of this type. Table 5 lists the interatomic distances arranged according to coordination number. The superscript numerals indicate the number of times a symmetrically equivalent distance is found (when reading down), and an asterisk indicates a 'major ligand' distance. In the *X* phase, 63% of the atoms have CN12, 5% CN14, 5% CN15 and 27% CN16. These percentages are not too different from those found in the Friauf–Laves–Komura phases, namely 66% CN12 and 33% CN16. This close relationship is also apparent in the secondary net of the *X* phase (Fig. 2), which could be transformed into a net with only 3^6 tessellations (such as occurs in the Friauf–Laves–Komura phases) by moving atoms 2 together, towards the symmetry center and atoms 3, farther apart.

Although the relative distribution of the Co and Mn atoms over the various positions could not be established in this study, it is clearly shown that the silicon atoms are not randomly distributed over the CN12 positions in this structure. Three of the nine CN12 positions are predominantly occupied by Si atoms, and one position is almost 50% occupied by Si. As was also found in the *v* phase (Shoemaker & Shoemaker, 1971), there are no Si atoms present in the first coordination shell around the 'Si only' positions. This may indicate a significant ionic charge on the Si atoms, presumably positive in agreement with the demonstrated small size of the Si atom (the average CN12–CN12 distance in the *X* phase is 2·372 Å).

Although occupancies of positions assumed not to contain silicon were not refined, the fact that the refined isotropic temperature factors fall within a reasonably narrow range lends support to our assumption that silicon is essentially confined to those four positions.

The requirements of a 'major skeleton' as discussed by Frank & Kasper (1959) are met, in the case of the *X* phase, by a single, three-dimensionally connected framework (Fig. 3).

Note added on 21 *September* 1971.

It has now come to our attention that the structure of the *X* phase has been determined independently by Yarmolyuk, Kripyakevich & Hladyshevskii (1970) from photographic data. These authors obtained the trial structure from Patterson sections, and refined it by *hk*0 electron-density projections to a final *R* index of 0·155 for 135 observed *hk*0 reflections. The structure is essentially the same as that derived by us, but individual differences in positional parameters are as large as 0·13 Å; the largest difference in an interatomic distance is 0·28 Å. All intermediate atoms were assumed to be at $z=0{\cdot}25$, and all CN12 positions were assumed to contain the same mixture of Mn, Co, and Si atoms; all other positions were assumed to contain Mn.

The authors express their appreciation to Dr Alan Parkes for his assistance in the data collection, to Professor Robert Ogilvie for his assistance with the electron microprobe work, to Dr Stephen Nagy for the chemical analysis, and to Professor Paul A. Beck for providing the *Q*-phase material. The authors also wish to express their appreciation to those who provided copies of the computer programs used in this work: Yvon, Jeitschko, & Parthé (powder simulation program); Ibers, Hamilton & Parkes (*PICK* 1 lattice and orientation refinement); Dewar & Stone (*FAME* and *MAGIC* symbolic-addition program); J. M. Stewart (*XRAY*67 program system) and Lee, Day & Knox (*ABSCOR* absorption correction program).

References

BARDOS, D. I., MALIK, R. K., SPIEGEL, F. K. & BECK, P. A. (1966). *Trans. A.I.M.E.* **236**, 40.

FRANK, F. C. & KASPER, J. S. (1958). *Acta Cryst.* **11**, 184.

FRANK, F. C. & KASPER, J. S. (1959). *Acta Cryst.* **12**, 483.

International Tables for X-ray Crystallography (1962). Vol. III, p. 215. Birmingham: Kynoch Press.

KARLE, J. & HAUPTMAN, H. (1953). *Solution of the Phase Problem. I. The Centrosymmetric Crystal*, ACA Monograph No. 3. The American Crystallographic Association.

KARLE, J. & KARLE, I. (1966). *Acta Cryst.* **21**, 849.

KUZ'MA, YU. B. (1962). *Russ. J. Inorg. Chem.* **7**, 691.

KUZ'MA, YU. B. & HLADYSHEVSKII, E. I. (1964). *Russ. J. Inorg. Chem.* **9**, 373.

PEARSON, W. B. & SHOEMAKER, C. B. (1969). *Acta Cryst.* B**25**, 1178.

SHOEMAKER, C. B. & SHOEMAKER, D. P. (1969). In *Developments in the Structural Chemistry of Alloy Phases*, p. 117. Edited by B. C. GIESSEN. New York: Plenum Press.

SHOEMAKER, C. B. & SHOEMAKER, D. P. (1971). *Acta Cryst.* B**27**, 227.

SHOEMAKER, D. P. & SHOEMAKER, C. B. (1968). In *Structural Chemistry and Molecular Biology*, p. 723. Edited by A. RICH & N. DAVIDSON. San Francisco: Freeman.

YARMOLYUK, YA. P., KRIPYAKEVICH, P. I. & HLADYSHEVSKII, E. I. (1970). *Kristallografiya*, **15**, 268. (*Sov. Phys.–Crystallogr.* **15**, 226.)